

Band-dropping via coupled photonic crystal waveguides

Mehmet Bayindir and Ekmel Ozbay

*Department of Physics, Bilkent University, Bilkent, 06533 Ankara,
Turkey*

bayindir@fen.bilkent.edu.tr

<http://www.fen.bilkent.edu.tr/bayindir>

Abstract: We observe the dropping of electromagnetic waves having a specific frequency or a certain frequency band in two-dimensional dielectric photonic crystals. The single frequency is dropped via cavity-waveguide coupling. Tunability of the demultiplexing mode can be achieved by modifying the cavity properties. The band-dropping phenomenon is achieved by introducing interaction between an input planar, or coupled-cavity, waveguide and the output coupled-cavity waveguides (CCWs). The dropping band can be tuned by changing the coupling strength between the localized cavity modes of the output CCWs. We also calculate the transmission spectra and the field patterns by using the finite-difference-time-domain (FDTD) method. Calculated results agree well with the microwave measurements.

© 2002 Optical Society of America

OCIS codes: (060.4230) Multiplexing; (230.7370) Waveguides; (230.5750) Resonators

References and links

1. J. D. Joannopoulos, R. D. Meade, and J. N. Winn, *Photonic Crystals: Molding the Flow of Light* (Princeton University Press, Princeton, NJ, 1995).
2. C. M. Soukoulis, ed., *Photonic Crystals and Light Localization in the 21st Century* (Kluwer, Dordrecht, 2001).
3. A. Mekis, J. C. Chen, I. Kurland, S. Fan, P. R. Villeneuve, and J. D. Joannopoulos, "High transmission through sharp bends in photonic crystal waveguides," *Phys. Rev. Lett.* **77**, 3787–3790 (1996).
4. M. Bayindir, B. Temelkuran, and E. Ozbay, "Propagation of photons by hopping: A waveguiding mechanism through localized coupled-cavities in three-dimensional photonic crystals," *Phys. Rev. B* **61**, R11855–R11858 (2000).
5. M. Loncar, D. Nedeljkovic, T. Doll, J. Vuckovic, A. Scherer, and T. P. Pearsall, "Waveguiding in planar photonic crystals," *Appl. Phys. Lett.* **77**, 1937–1939 (2000).
6. O. Painter, R. K. Lee, A. Scherer, A. Yariv, J. D. O'Brien, P. D. Dapkus, and I. Kim, "Two-dimensional photonic band-gap defect mode laser," *Science* **284**, 1819–1821 (1999).
7. S. Noda, M. Yokoyama, M. Imada, A. Chutinan, and M. Mochizuki, "Polarization mode control of two-dimensional photonic crystal laser by unit cell structure design," *Science* **293**, 1123–1125 (2001).
8. J. Yonekura, M. Ikeda, and T. Baba, "Analysis of finite 2-D photonic crystals of columns and lightwave devices using the scattering matrix method," *J. Lightwave Technol.* **17**, 1500–1508 (1999).
9. M. Bayindir, B. Temelkuran, and E. Ozbay, "Photonic crystal based beam splitters," *Appl. Phys. Lett.* **77**, 3902–3904 (2000).
10. J. C. Knight, J. Broeng, T. A. Birks, and P. S. J. Russell, "Photonic band gap guidance in optical fibers," *Science* **282**, 1476–1479 (1998).
11. H. Kosaka, T. Kawashima, A. Tomita, M. Notomi, T. Tamamura, T. Sato, and S. Kawakami, "Photonic crystals for micro lightwave circuits using wavelength-dependent angular beam steering," *Appl. Phys. Lett.* **74**, 1370–1372 (1999).

12. A. de Lustrac, F. Gadot, S. Cabaret, J.-M. Lourtioz, T. Brillat, A. Priou, and A. E. Akmansoy, "Experimental demonstration of electrically controllable photonic crystals at centimeter wavelengths," *Appl. Phys. Lett.* **75**, 1625–1627 (1999).
 13. P. R. Villeneuve, D. S. Abrams, S. Fan, and J. D. Joannopoulos, "Single-mode waveguide microcavity for fast optical switching," *Opt. Lett.* **21**, 2017–2019 (1996).
 14. S. Fan, P. R. Villeneuve, J. D. Joannopoulos, and H. A. Haus, "Channel drop tunneling through localized states," *Phys. Rev. Lett.* **80**, 960–963 (1998).
 15. S. Noda, A. Chutinan, and M. Imada, "Trapping and emission of photons by a single defect in a photonic bandgap structure," *Nature* **407**, 608–610 (2000).
 16. B. E. Nelson, M. Gerken, D. A. B. Miller, R. Piestun, C.-C. Lin, and J. S. Harris, "Use of a dielectric stack as a one-dimensional photonic crystal for wavelength demultiplexing by beam shifting," *Opt. Lett.* **25**, 1502–1504 (2000).
 17. S. S. Oh, C.-S. Kee, J.-E. Kim, H. Y. Park, T. I. Kim, I. Park, and H. Lim, "Duplexer using microwave photonic band gap structure," *Appl. Phys. Lett.* **76**, 2301–2303 (2000).
 18. M. Koshiba, "Wavelength division multiplexing and demultiplexing with photonic crystal waveguide couplers," *J. Lightwave Technol.* **19**, 1970–1975 (2001).
 19. A. Sharkawy, S. Shi, and D. W. Prather, "Multichannel wavelength division multiplexing with photonic crystals," *Appl. Opt.* **40**, 2247–2252 (2001).
 20. C. Jin, S. Han, X. Meng, B. Cheng, and D. Zhang, "Demultiplexer using directly resonant tunneling between point defects and waveguides in a photonic crystal," *J. Appl. Phys.* **91**, 4771–4773 (2002).
 21. M. Bayindir and E. Ozbay, "Dropping of electromagnetic waves through localized modes in three-dimensional photonic band gap structures," Submitted to *Appl. Phys. Lett.*
 22. E. Ozbay, M. Bayindir, I. Bulu, and E. Cubukcu, "Investigation of localized coupled-cavity modes in two-dimensional photonic band gap structures," *IEEE J. Quantum Electron.* **38**, 837–843 (2002).
 23. M. Bayindir, B. Temelkuran, and E. Ozbay, "Tight-binding description of the coupled defect modes in three-dimensional photonic crystals," *Phys. Rev. Lett.* **84**, 2140–2143 (2000).
-

1. Introduction

Photonic crystals, in which the propagation of electromagnetic waves is forbidden for a certain frequency range, provide a promising tool to control the flow of light in integrated optical devices [1, 2]. In the last several years, there is a great deal of interest in developing photonic crystal based components such as waveguides [3, 4, 5], lasers [6, 7], splitters [8, 9], fibers [10], optical circuits [11, 12], and ultrafast optical switches [13].

Photonic band gap structures can also be used to construct the optical add-drop filters which can be effectively used in wavelength-division-multiplexing (WDM) applications. The first photonic crystal based WDM structure was proposed by Fan *et. al.* by using resonant tunneling phenomena between two line-defect waveguides via cavities [14]. Kosaka *et. al.* reported WDM filters by using superprism phenomena [11]. Noda and his co-workers proposed and experimentally demonstrated trapping and dropping of photons via cavity-waveguide coupling in 2D photonic crystal slabs [15]. Nelson *et. al.* reported wavelength separation by using 1D dielectric multilayer stacks [16]. Moreover, various types of WDM structures in 2D photonic crystals have also been reported [17, 18, 19, 20]. Recently, we achieved dropping of electromagnetic waves in three-dimensional (3D) layer-by-layer photonic crystals [21].

In this paper, we propose and demonstrate the band-demultiplexing phenomenon in 2D photonic crystals. The single frequency dropping is achieved via coupling between resonant cavities and a waveguide [See Fig. 1(a)]. The tunability of the dropping frequency is obtained by changing the properties of the cavities, i. e., volume or effective dielectric constant of the cavities. The band-dropping phenomenon is demonstrated by using coupled waveguide structures as shown in Fig. 1(b). The input port consists of either a planar waveguide (PW) or a coupled-cavity waveguide (CCW). The output ports consist of two or more noninteracting CCWs.

We constructed a 2D photonic crystal which consists of 20×30 square array of dielectric cylindrical alumina rods having radius $r_0 = 1.55$ mm and refractive index

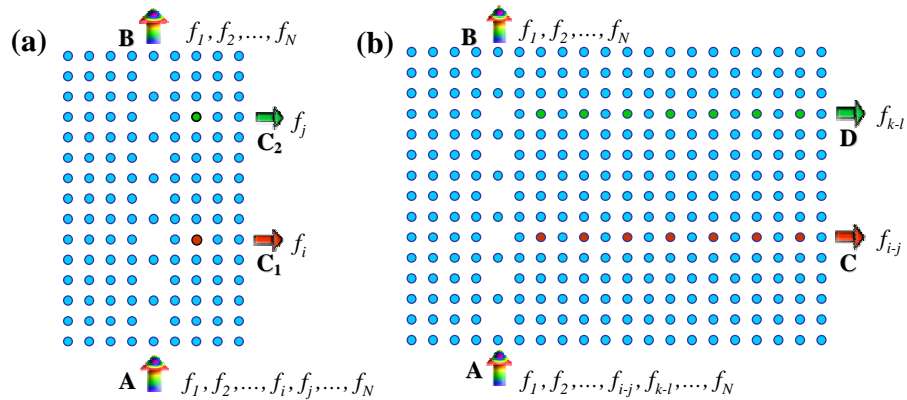


Fig. 1. Dropping of electromagnetic waves in two-dimensional photonic crystals. (a) Schematic drawing of a single-frequency dropping structure. A selected frequency can be dropped from the guided mode inside the waveguide due to coupling between the cavity and the waveguide mode. The tunability of the dropping frequency can be achieved by changing radius of the rods at the cavity sites. (b) The proposed band-demultiplexing structure. Photons having a certain frequency band inside the input waveguide can be filtered through the output coupled-cavity waveguides.

$n = 3.1$ at the microwave frequencies. The lattice constant and the corresponding filling fraction are $a = 8$ mm and $\eta \sim 0.12$, respectively. Length of the rods is 150 mm which is almost two order of magnitude larger than the operation wavelengths. The experimental set-up consisted of a HP 8510C network analyzer and microwave horn antennas to measure the transmission-amplitude properties. The transverse magnetic (TM) polarization where the incident electric field was parallel to the rods, is considered in all measurements. It is well known that the other polarization, transverse electric (TE), does not produce any photonic band gaps in this frequency range [1]. The crystal exhibits a photonic band gap between the normalized frequencies $0.26c/a$ to $0.45c/a$, where c is the speed of light.

The transmission spectra and the field patterns are obtained by using a finite-difference-time-domain (FDTD) code [22]. In our experiments, normalization of the transmission data is done as follows. First, we measure the transmission spectra in the free space (i. e., without photonic crystal). This data is used as the calibration data for the network analyzer. Then, we insert the crystal between the horn antennas, and we perform the transmission measurements by keeping the distance between transmitter and receiver antennas fixed. In FDTD simulations, we normalize the transmission spectra with respect to the source spectra.

2. Single Frequency Dropping

In order to demonstrate the single-frequency demultiplexing [15, 19, 20], we construct two different cavity-waveguide coupling configurations. First structure consists of a planar waveguide (PW), which is formed by removing a row of rods [3], and cavities [See Fig. 2 (right panel)]. The cavities are generated by replacing the rods at the cavity sites with thinner rods. This results in acceptor-like cavities that are coupled to the waveguide. Figure 2(a) and (b) display the simulated and measured transmission characteristics as function of normalized frequency, respectively. The spectra show that the demultiplexing frequency is shifted towards lower frequencies as we increase the radius of the rods at cavity sites. The simulated resonant frequencies are $f = 0.391c/a$, $0.373c/a$, and $0.352c/a$ for $r_c = 0$, $r_c = 0.32r_0$, and $r_c = 0.48r_0$, respectively. The corresponding

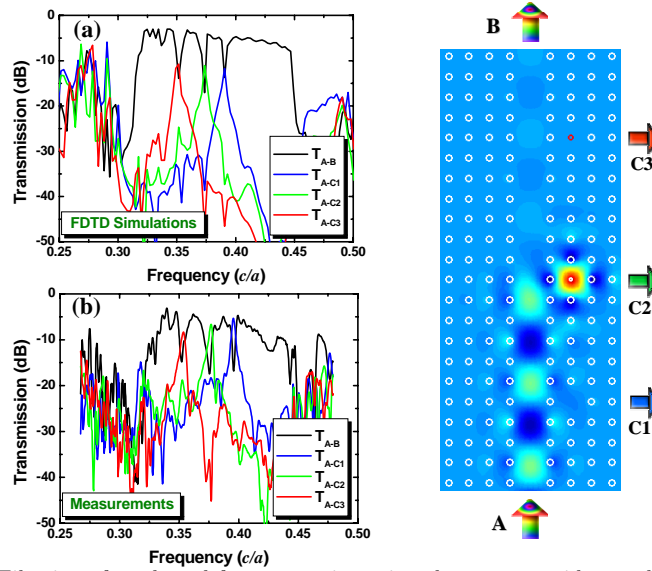


Fig. 2. Filtering of a selected frequency via cavity-planar waveguide coupling. [Left panel] (a) Calculated and (b) measured transmission spectra, $A \rightarrow C$, corresponding to the single-frequency demultiplexing structures for various values of $r_c = 0$ (blue line), $r_c = 0.32r_0$ (green line), and $r_c = 0.48r_0$ (red line). Tunability of the dropping frequencies can be achieved by changing radius of the rods at the cavity sites. The waveguide spectrum (black line, $A \rightarrow B$) exhibits corresponding dips exactly at the resonance frequency of cavities. [Right panel] Calculated field pattern at the resonance frequency of the cavity C2. The electric field distribution clearly shows the filtering of cavity mode from the waveguide mode.

measured frequencies are $f = 0.395c/a$, $0.377c/a$, and $0.353c/a$ which are very close to the calculated results. The transmission spectrum of the PW exhibits dips exactly at these resonant frequencies. As shown in Fig. 2 (right panel), we also calculate the field distribution at $f = 0.373c/a$. The field pattern clearly shows the dropping of the cavity mode from the waveguide mode. We construct a second structure by replacing the PW with a CCW as shown in Fig. 3 (right panel). For this configuration, simulated [Fig. 3(a)] and measured [Fig. 3(b)] results are in good agreement, and very similar results are obtained as in the previous case. However, the dropping efficiency is not so high in the second configuration compared to the first configuration.

It is important to note that by using the method reported by Fan and his co-workers, we can increase the transmission amplitude of the dropping mode [14]. By introducing an accidental degeneracy into the system (for example by using two weakly interacting cavities), one can achieve a complete dropping for the resonant mode.

3. Band Dropping

Next, we construct two different band-demultiplexing structures. First configuration consists of an input PW and two output CCWs, which are coupled to the PW as shown in Fig. 4 (right panel). The bandwidth of the waveguiding band of a CCW is proportional to the coupling constant, κ , and the single cavity resonant frequency Ω_0 , which is given by $\Delta\omega = 2\kappa\Omega_0$ [22, 23]. In addition, the waveguiding band is centered around Ω_0 . Keeping in mind these properties, we construct the output CCWs by using two different cavity arrays with cavity rod radii are $r_c = 0.32r_0$ and $r_c = 0.64r_0$. The simulated transmission spectra of this configuration are presented in Fig. 4(a). The guiding band of the PW is extending from $f = 0.314c/a$ to $f = 0.454c/a$. Corresponding

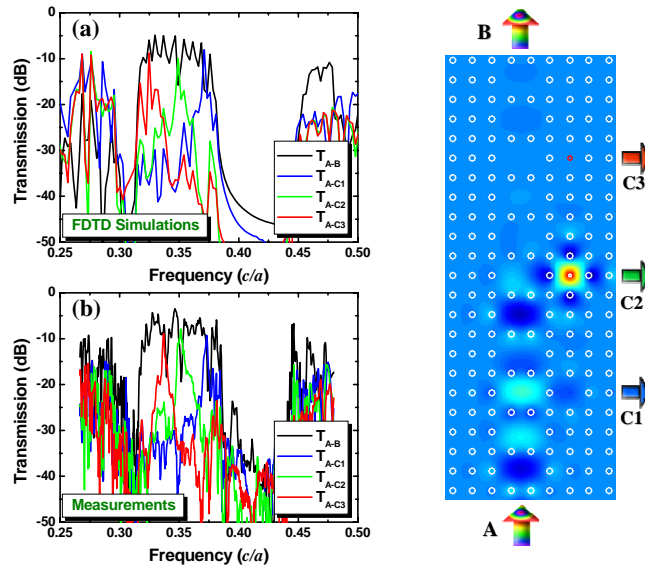


Fig. 3. Filtering of a selected frequency via cavity-coupled cavity waveguide coupling. [Left panel] (a) Calculated and (b) measured transmission spectra corresponding to the single-frequency demultiplexing structures for various values of $r_c = 0$ (blue line), $r_c = 0.32r_0$ (green line), and $r_c = 0.48r_0$ (red line). The black line represents the corresponding transmission spectrum of the coupled-cavity waveguide. [Right panel] Calculated field pattern at the resonance frequency of the cavity C2.

guiding bands for CCWs are extending from $f = 0.314c/a$ and $0.355c/a$ to $f = 0.337c/a$ and $0.391c/a$ for $r_c = 0.64r_0$ and $r_c = 0.32r_0$, respectively. The measurements give very similar results as shown in Fig. 4(b). Demultiplexing of the CCWs bands from the PW mode are more apparent in the measured spectra. We also plot the field distribution for $f = 0.369c/a$ in Fig. 4 (right panel). The field pattern exhibits the dropping of the corresponding mode from the PW mode.

The second configuration is obtained by replacing the PW with a CCW which is constructed by an array of coupled cavities with two missing rods [See Fig. 5 (right panel)]. In this case, the simulation results in a guiding band for the input CCW between $f = 0.311c/a$ and $f = 0.381c/a$. The guiding band for the output CCWs are extending from $f = 0.311c/a$ and $0.353c/a$ to $f = 0.339c/a$ and $0.383c/a$ for $r_c = 0.64r_0$ and $r_c = 0.32r_0$, respectively [See Fig. 5(a)]. In experiments, we obtain similar results as displayed in Fig. 5(b). Figure 5 (right panel) also shows the field distribution for $f = 0.363c/a$, where we again observe the dropping of a frequency within the second CCW band.

4. Conclusion

In summary, we demonstrated a method for band-demultiplexing phenomenon in photonic band gap structure. Dropping of selected frequency band was achieved from input waveguide mode through output coupled-cavity waveguides. Our results might be important for designing future ultrasmall photonic crystal based demultiplexing components in optical circuits.

This work was supported by NATO Grant No. SfP971970, and European Union Project EU-DALHM.

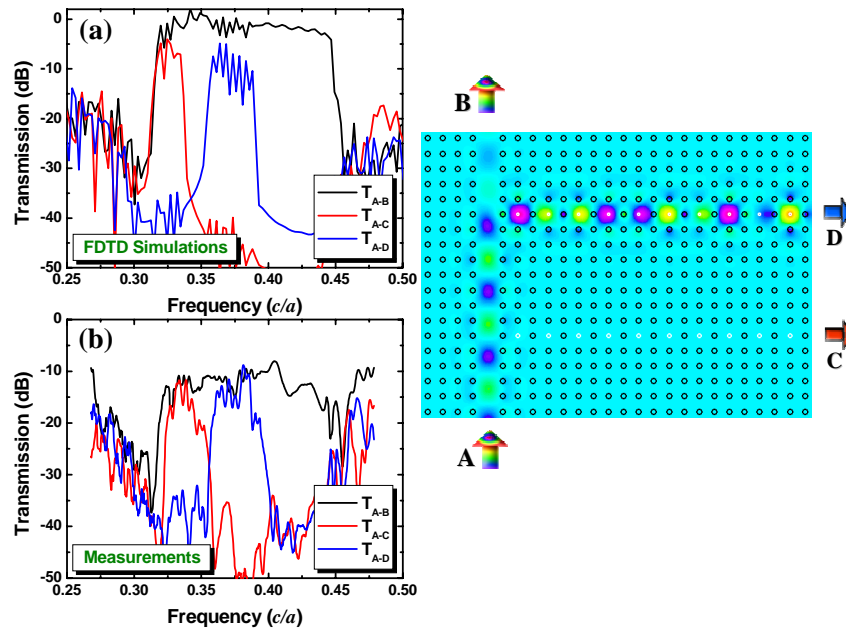


Fig. 4. Band-dropping from an input planar waveguide through output coupled-cavity waveguides. [Left panel] (a) Calculated (b) measured transmission spectra corresponding to the band-demultiplexing structure which contains two CCWs with the cavity rod radius $r_c = 0.32r_0$ (blue line) and $r_c = 0.64r_0$ (red line). [Right panel] Calculated field distribution for frequency $f = 0.369c/a$.

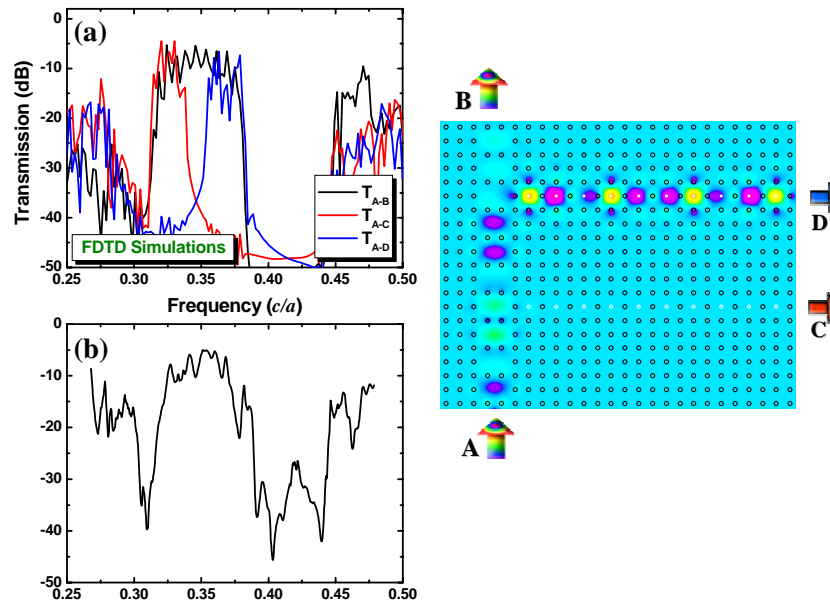


Fig. 5. Band-dropping from an input coupled-cavity waveguide through output coupled-cavity waveguides. [Left panel] (a) Calculated (b) measured transmission spectra corresponding to the band-demultiplexing structure which contains two CCWs with the cavity rod radius $r_c = 0.32r_0$ (blue line) and $r_c = 0.64r_0$ (red line). [Right panel] Calculated field distribution for frequency $f = 0.363c/a$.